www.saber.ula.ve/avancesenquimica
Avances en Química, 14(3), 89-96 (2019)
Artículo científico

XAES studies of three samples of natural aluminosilicates

J. Mendialdua[1], R. Casanova[1*], Fulgencio Rueda[1], Alfonso Rodríguez[1], Issam Taebi[2], Louise Jalowiecki[2], José A. Lobo B.[1], José C. Valera[1], Ela Michelangeli[1]

[1)] Laboratorio de Física de Superficies. Dpto. de Física. Fac. de Ciencias. ULA. Mérida 5101.Venezuela.

[2)] Laboratoire de Catalyse Héterogène, U.R.A.C.N.R.S. No 402, Université des Sciences et Techniques de Lille Flandres-Artois. 59655 Villeneuve d´Ascq Cedex, France.

(*) rodrigoc@ula.ve

Recibido: 17/02/2019 **Revisado**: 17/05/2019 **Aceptado**: 30/12/2019

Resumen

El uso potencial de la espectroscopia XAES para la identificación de estados químicos en la superficie ha sido demostrado una vez más en este trabajo. Para este propósito, la información contenida en el parámetro Auger modificado, junto con sus corrimientos y su relación directa con la energía de correlación hueco-hueco ha sido explotada exitosamente. El análisis detallado de la región del Auger KLL del oxígeno nos ha permitido caracterizar las muestras SLB1, VL1 and ULA1 al comparar esta región con la del Fe_2O_3, Al_2O_3, SiO_2 y una mezcla mecánica de estos óxidos. También hemos establecido claramente que las superficies de SLB1 y VL1 no son mezclas de óxidos, en acuerdo con nuestros trabajos previos de XPS.

Palabras claves: XAES; parámetro Auger; óxidos; energía de correlación

Abstract

The potential use of XAES (X-ray excited Auger Electron Spectroscopy) for surface chemical states identification has been shown once more in this work. For this purpose, the information contained in the modified Auger parameter, together with its shifts and its direct relationship to the hole-hole correlation energy has been exploited successfully. The detailed analysis of the oxygen Auger KVV region has allowed us to characterize three natural aluminosilicate samples SLB1, VL1 and ULA1 by comparing this region to that of Fe_2O_3, Al_2O_3 and SiO_2 and a mechanical mixture of these oxides. We have also clearly established that the surfaces of two of the aluminosilicates studied are not oxide mixtures, in agreement with our previous XPS works.

Keywords: XAES; Auger parameter; Oxides; Correlation energy

Introduction

The potential use of X-ray excited Auger electron spectroscopy (XAES) to identify surface chemical states in many substances has been shown by several authors[1,6]. The spectra registering Auger transitions with valence level final states, e.g. the KVV transitions for oxygen, are the most appropriate for this identification since these levels are very sensitive to the local atomic environment[1,2]. The Auger parameter introduced by Wagner[1,7-9] the modified Auger parameter[10,11] which contain a great deal of information, together with the Auger parameter shifts and their direct relation to the hole-hole correlation energy values[12-14] have been used for characterizing chemical states of many substances. Our laboratory has dedicated a good effort to surface characterization of transition metal oxides, zeolites and catalysts based on substances with aluminum-oxygen, iron-oxygen and silicon-oxygen bonds using mainly X ray photoelectron spectroscopy[15-18].

In this work, results related to their chemical state, obtained by X-ray excited Auger electron spectroscopy, on several compounds are reported. Attention is focused on the oxygen KLL Auger region to acquire information given by the parameters mentioned previously and exploit the shape and structure exhibited by this region. Being oxygen a light element, its KLL spectrum can be explained in the LS coupling scheme[19]. According to this, the possible Auger transitions are denoted as KL_1L_1 ($^1S_0$), KL_1L_2 ($^1P_3$), KL_1L_3 (^3P), KL_2L_2 ($^1S_0$), KL_2L_3 ($^1D_2$); the last two transitions are frequently denoted by KVV because the two holes in the final state are in the valence band. The oxygen KVV region contains more information about the surface than the O 1s region due to the energy dependence of the mean free path λ, which is sensitive to surface contamination. The samples studied in this report correspond to three natural aluminosilicates (designated from now on as ULA1, VL1 and SLB1) and a mechanical mixture (mixture M) of the oxides Fe_2O_3, Al_2O_3 and SiO_2 with a 4:2:1 weight proportion respectively. For comparison purposes, some results of the above mentioned oxides are also included; assuming that if the natural samples are mixtures of these oxides, their Auger spectra should resemble to those obtained from the proper linear combinations of these oxide spectra.

Experimental

Samples

In this work we have studied three natural aluminosilicates reported in previous works[20-24]: the certified sample VL1 with a proposed content of SiO_2 (1.16 wt.%), Al_2O_3 (37.38 wt.%), Fe_2O_3 (35.72 wt.%), TiO_2 (3.15 wt.%) LOI (22.54 %)[20]; the certified sample SLB1 with a proposed composition of: SiO_2 (1.93 wt. %), Al_2O_3 (45.50 wt.%), Fe_2O_3 (24.03 wt.%), TiO_2 (1.75 wt.%) LOI (26.79 %)[21], both samples analyzed before and after being used in catalytic tests in oxidative dehydrogenation of propane to propene; the third material is a natural catalyst (ULA1) composed[22] by Fe (62.55 wt.%), Al (0.40 wt.%), Si (14.20 wt.%), Ti (0.10 wt.%); which was analyzed before and after being used as a catalyst in hydrocarbon synthesis. The samples used in catalytic reactions were placed into the XPS spectrometer, after being exposed to atmospheric conditions. For identification purposes a sample studied before or after a catalytic test will be designated sample BT or sample AT respectively. The samples were analyzed in the temperature range from 523 to 773 K. Ultra pure oxides samples: Fe_2O_3, SiO_2, Al_2O_3 were also analyzed as well as a mechanical mixture (mixture M) with a 4:2:1 weight proportion (equivalent to 57.14 wt.% Fe_2O_3, 28.57 wt.% Al_2O_3, and 14.28 wt.% SiO_2).

We also include previous results of an ultra pure sample of MgO for comparison of the Auger structures and because in its spectrum the structures assigned by Wagner[1] and Fuggle[2] can be clearly observed. In all the tables and in figure 5h we include our results, which differ to those of Wagner but agree to those of Fuggle.

XAES measurements

A VSW spectrometer with a preparation chamber and Ar^+ ion etching facilities was used for this work in conjunction with a Leybold LHS 10S spectrometer whose specifications can be found elsewhere[16,18]. Vacuum in the spectrometers, during measurements, was in the 10^{-9}mbar range. Its hemispherical analyzer was operated at constant pass energy of 22.4 eV. Non-monochromatic Al Kα radiation was employed as X-ray photon source with a constant 300 watts power. The C1s binding energy at 285.0 eV of adventitious carbon was used, whenever possible, as an acceptable binding energy reference; however, when the intensity of this peak was very low (after ion etching), the Al 2p level binding energy in Al_2O_3 (74.6 eV) or the Si 2p binding energy in SiO_2 (103.8 eV) were used as internal energy references, depending on the sample under study. The mechanical mixture and ULA1 sample exhibited a differential charge effect[18,24] which leads to inaccuracies on determining the binding energies, but this can be solved taking internal references like the Si 2p binding energy (103.8 eV) for the peaks originating from the sample physical region consisting of SiO_2, the O 1s binding energy (530.3 eV) for the oxygen bonded to iron for those XPS peaks rising from the sample physical region consisting of Fe_2O_3 , and the Al 2p level (74.6 eV) for the peaks originating from the sample region consisting of Al_2O_3.

Samples were mounted as reported previously[22-24]. Each sample, depending on the spectrometer used, was subjected to a sequence of sample treatments performed in the spectrometer preparation chamber, as shown in table 1. Ion bombardment was done with 3 KeV Ar^+ ions in 15 minutes cycles. Annealing was done in vacuum at 773 K for approximately 6 hours. Both treatments, the hydrogen reduction (in 1x 10^{-5} mbar of H_2) and re-oxidation (in 1x 10^{-5} mbar of O_2), were performed in the spectrometer preparation chamber at 773 K for a period between 4-20 hours depending on the sample under study.

Due to their hygroscopic nature, all the samples (excepting VL1 BT, SLB1BT, SiO_2 and Al_2O_3) were heated at 423 K before introducing them into the analysis chamber in order to preserve its vacuum. For this reason, VL1 BT and SLB1 BT samples were calcined due to the high content of interstitial water. SiO_2 and Al_2O_3 were also calcined before XPS analysis. The calcination period done at 773 K lasted between 5 and 12 hours depending on the sample.

The procedures to exploit quantitatively the spectra are given in detail in Mendialdua *et al*.[25] and other works of our lab.

Results and discussion

In order to make easier the presentation of our results and their discussion, we present here the definition of the Auger parameters α′ and β′. According to Moretti[13] and for the case of oxygen:

$$\alpha' = E_k (KL_{23}L_{23}) + E_b (O\ 1s) \quad (1)$$

$$\beta' = E_k (KL_1L_{23}) + E_b (O\ 1s) \quad (2)$$

where $E_k (KL_{23}L_{23})$ and $E_k (KL_1L_{23})$ are the kinetic energies due to the Auger electrons originated for the electron transitions in parenthesis. To obtain the values for the shifts Δα′ and Δβ′of these Auger parameters, with respect to water in the gas phase, we make the difference between α′ or β′ for each sample and the corresponding value α′ or β′ for water. We have taken from the literature[13] the following reference values for α′ and β′: α′= 1038.5 eV and β′= 1014.5 eV corresponding to transitions $KL_{23}L_{23}$ and KL_1L_{23} for water in gas phase, while U(2p2p) and U(2s2p) can be calculated as follows:

$$U(2p2p) \approx 8.5 - \Delta\alpha' \quad (3)$$

and

$$U(2s2p) \approx 16.5 - \Delta\beta' \quad (4)$$

with U(2p2p) and U(2s2p) the hole-hole repulsion energies in the final state. The calculated values for the Auger parameters will be presented in table 1, while their shifts and the energies U(2p2p) and U(2s2p) will be given in table 2.

Sample SLB1

According to its composition this sample should have a $N_{Al}/N_{Fe} \approx 3$ bulk concentration ratio, while the XPS surface analysis gives a 3.9 ratio for the SLB1 BT reoxidized sample, indicating an Al surface enrichment.

Oxygen Auger spectra corresponding to transitions KL_1V to KVV (KL_1L_{23} to $KL_{23}L_{23}$) for SLB1, Al_2O_3 and Fe_2O_3 are shown in figure 1, where the ordinate scale has been normalized to one for the maximum value of each spectrum. The oxygen Auger region for SLB1 does not exhibit, on the high energy side of the $KL_{23}L_{23}$ transition, the obvious structure shown by Al_2O_3 in this region. The KL_1L_{23} transition peak has a less defined structure than in Al_2O_3 and Fe_2O_3.

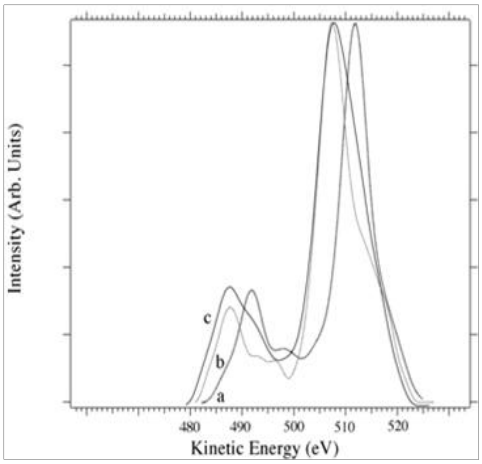

Fig. 1: O KLL Auger spectra from: a) Fe_2O_3, b) Al_2O_3, c) SLB1 sample.

One might think that SLB1 is a mixture of Al_2O_3 and Fe_2O_3; however, a linear combination of spectra (see figure 2, with the ordinate scale normalized to one) for Al_2O_3 and Fe_2O_3, using the proper coefficients obtained from the bulk and surface N_{Al}/N_{Fe} ratios, does not correspond to the SLB1 spectrum obtained experimentally. Comparing the values of the Auger

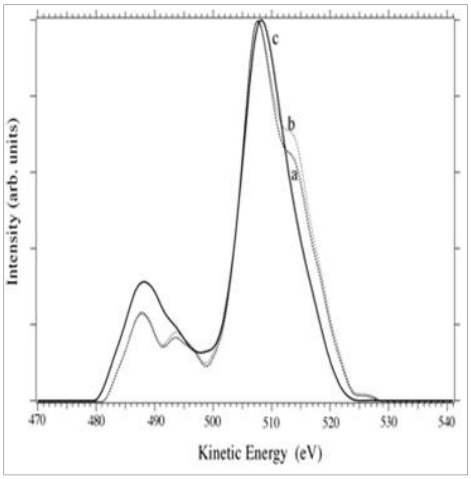

Fig. 2: Comparison of oxygen Auger region for sample SLB1, obtained from a linear combination of spectra for Al_2O_3 and Fe_2O_3 using the proper coefficients obtained from a) the surface N_{Al}/N_{Fe} ratio, b) the bulk N_{Al}/N_{Fe} ratio, with c) experimental oxygen Auger region for sample SLB1.

parameters and their shifts for SLB1 with those of Al_2O_3 and Fe_2O_3 (see tables 1 and 2) it can be seen that the values of α' and $\Delta\alpha'$ are close to those of SiO_2 despite its composition; the values of β' and $\Delta\beta'$ are closer to those of Al_2O_3. Analogously, the values of the hole-hole correlation energies U(2p2p) and U(2s2p) are close to those of Al_2O_3. However, the less defined KL_1L_{23} structure indicates a valence band structure different to Al_2O_3 and Fe_2O_3.

It appears that SLB1 is composed of iron aluminate predominating over the aluminum and iron oxides. This is consistent with the inertness of this sample to different sample treatments in contrast with the reactivity exhibited by Fe_2O_3, whether alone or in a mechanical mixture with SiO_2 and Al_2O_3, under the same conditions; this supports the fact that iron in SLB1 is in a higher stability state than that shown in Fe_2O_3. However, SLB1 experiences a transformation once it is subjected to catalytic tests in oxidative dehydrogenation reactions of propane into propene[26], since its modified Auger parameter (see table 1) has a value close to that of alumina.

Sample VL1

According to its composition, this sample has a $N_{Al}/N_{Fe} = 1.7$ bulk concentration ratio, while the XPS data gives a surface concentration ratio $N_{Al}/N_{Fe} = 1.0$ indicating Al depletion on the surface region. No carbonates were detected by XPS in the C 1s region and the intensity of the CO region is very low, indicating a very small contribution of this oxygen in the Auger region.

A comparison of the oxygen Auger region for VL1, Al_2O_3, and Fe_2O_3 is shown in figure 3. A suitable linear combination of the Al_2O_3 and Fe_2O_3 spectra according to the N_{Al}/N_{Fe} ratios is shown in figure 4. From this figure, it is deduced that this sample is not an Al_2O_3, and Fe_2O_3 mixture. It is important to point out (see figure 5d) that the O1s peak shape does not correspond to that expected for the N_{Al}/N_{Fe} surface ratio. Its modified Auger parameter (1040.8) (see table 1, column 7) is completely different from that of alumina, iron oxide, lying between the two.

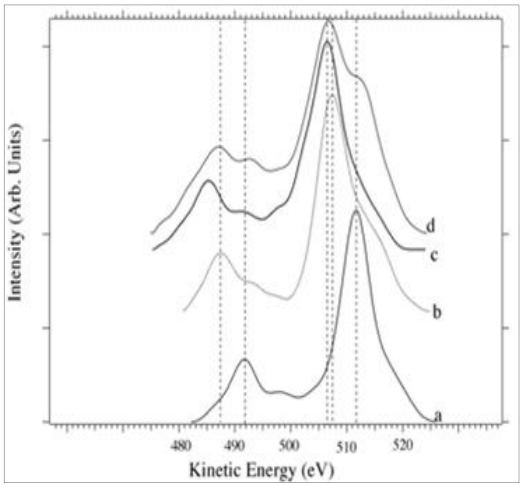

Fig. 3: O KLL Auger spectra of a) Al_2O_3, b) Fe_2O_3, c) sample VL1

Table 1. Photoelectron Auger line energy data and Auger parameters for different samples.

Sample	*KL_1L_2* E_k *(eV)*$\pm$*0.2*	*KL_2L_3* E_k *(eV)*$\pm$*0.2*	*KVV-KL_1L_2* *(eV)*	*O 1s* E_b*(eV)*$\pm$*0.1*	*O_{1s}-KVV* *(eV)*	*α'* *(eV)*	*β'* *(eV)*
SiO_2							
AR	485.3	506.6	21.3	532.8	26.2	1039.4	1018.1
Re-oxidized	485.3	506.6	21.3	532.8	26.2	1039.4	1018.1
Al_2O_3							
AR	487.3	507.3	20.0	531.4	24.1	1038.7	1018.7
H_2 reduced	487.7	507.5	19.8	531.3	23.8	1038.8	1019.0
Ion^+etched	487.2	507.2	20.0	531.6	24.4	1038.8	1018.8
Re-oxidized	487.7	507.3	19.6	531.3	24.0	1038.6	1019.0
Fe_2O_3							
AR	492.7	511.7	19.0	530.3	18.6	1042.0	1023.0
Calcined	492.4	512.0	19.6	530.3	18.3	1042.3	1022.7
H_2 reduced	492.6	511.6	19.0	530.3	18.7	1041.9	1022.9
Re-oxidized.	493.1	512.9	19.8	530.3	17.4	1043.2	1023.4
Mixt. M							
AR }	487.1 492.8 (*)	506.9 511.7	19.8 18.9(*)	533.2 529.7	26.3 18.0	26.3 18.0	1020.3 1022.5(*)
Re-oxidized }	487.1 492.5 (*)	507.8 512.3	20.7 19.8 (*)	532.6 529.2	24.8 16.9(*)	24.8 16.9(*)	1019.7 1021.7(*)
ULA1AT							
AR }	487.0 492.4(*)	507.2 512.4	20.2 20(*)	532.9 530.3	25.7 17.9(*)	1040.2 1042.8	1020.4 1022.8(*)
SLB1 BT							
AR	487.5	507.9	20.4	531.4	23.5	1039.3	1018.9
Annealed	487.8	508.2	20.4	531.4	23.2	1039.6	1019.2
Ion etched	487.6	508.2	20.6	531.4	23.2	1039.6	1019.0
Re-oxidized.	487.9	508.1	20.2	531.2	23.1	1039.3	1019.1
SLB1 AT							
AR	487.7	507.9	20.2	531.1	23.2	1039.1	1018.9
Ionetched	487.7	507.7	20.0	531.3	23.6	1039.1	1019.1
Annealed	487.6	508.0	20.4	530.9	22.9	1039.0	1018.6
Re-oxidized	488.5	508.3	19.8	530.6	22.3	1039.0	1019.2
VL1 BT							
AR	491.1	510.7	19.6	530.1	19.4	1040.8	1021.2
Ionetched	490.6	510.4	19.8	530.5	20.1	1040.9	1021.1
Annealed	490.7	510.5	19.8	529.6	19.1	1040.1	1020.3
Re-oxidized.	490.4	510.4	20.0	530.4	20.0	1040.8	1020.8
VL1 AT							
AR	490.8	510.8	20.0	530.1	19.3	1041.0	1021.0
Annealed	490.5	510.5	20.0	529.7	19.1	1040.3	1020.3
Ion etched	490.0	509.8	19.8	530.1	20.3	1040.0	1020.2
Re-oxidized	489.9	510.1	20.2	530.6	20.5	1040.8	1020.6
MgO							
AR	488.6	508.7	20.1	530.2	21.5	1038.9	1018.8
Re-oxidized	489.5	509.0	19.5	530.2	21.2	1039.2	1019.7

(*) values obtained from an estimation of the KL_1L_2 position in the oxygen bonded to iron.

AR: sample in the as received condition, BT : before catalytic tests, AT : after catalytic tests.

The spectral structure (see figure 5) does not permit obtaining two values for the Auger parameter, as can be done for ULA1 and mechanical mixture (MM) (see figures 5f and 5g respectively). The spectral region for the KL_1L_{23} transition does not show practically any structure, contrary to what it is observed for Al_2O_3 and Fe_2O_3. This evidence indicates the presence of some aluminate (and/or ferrate) on the sample's surface, different to that present on sample SLB1, also shown by the difference in the Auger parameters (see table 1) as well as in table 2, where it can be observed that the values of $\Delta\alpha'$ and

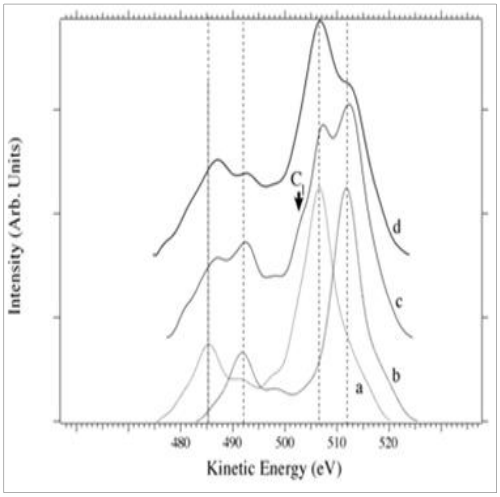

Fig. 4: Comparison of the oxygen Auger region for sample VL1, obtained from a linear combination of spectra Al_2O_3 and Fe_2O_3 using the proper coefficients given by a) the surface N_{Al}/N_{Fe} ratio, b) the bulk N_{Al}/N_{Fe} ratio, with c) experimental oxygen Auger region for sample VL1.

$\Delta\beta'$ differ from those of Fe_2O_3, Al_2O_3 and SiO_2; the hole-hole repulsion energies U(2p2p) and U(2s2p) are also very differ ent from those three samples. On the other hand, it can also be pointed out that VL1 responds differently to catalytic tests than SLB1.

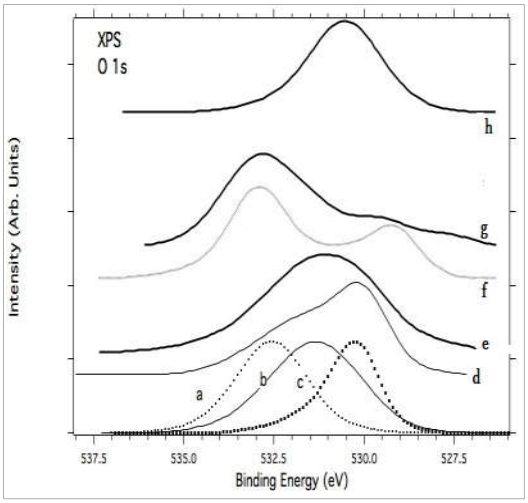

Fig. 5: O1s XPS spectral regions for samples: a) Fe_2O_3, b) Al_2O_3, c) SiO_2 AR, d) VL1, e) SLB1, f) ULA1 AT, g) mixture M AR, h) MgO.

Sample Mechanical Mixture

The oxygen Auger spectral region for Fe_2O_3, SiO_2, Al_2O_3 and mixture M is shown in figure 6. The structures related to the KL_1L_{23} region present in SiO_2, Al_2O_3 and Fe_2O_3 are also present in the mechanical mixture. In addition, the $KL_{23}L_{23}$ transition of oxygen bonded to both iron and silicon allows us to define two Auger parameters for this sample; one in the SiO_2 region and the other in the Fe_2O_3 region.

The mechanical mixture exhibits a differential charge effect between the silicon and iron physical regions, which was easily observed in the O 1s XPS peak; the C 1s peak spectrum for this sample has a FWHM remarkably superior than in Fe_2O_3, due to the differential charge effect. However, the low intensity of this spectrum, that indicates the low content of carbon in this sample, did not permit peak fitting. No carbonate signal was detected and the CO contribution was insignificant. The differential charge effect is also present in the Auger spectra, but does not affect the Auger parameters determination as expected. The spectrum g in figure 7 permits, by an approximate spectral decomposition, the determination of the energy values of the O KL_2L_3 transition in the corresponding region of SiO_2 and Fe_2O_3. These values are presented in table 1.

Table 2: Auger parameter shifts and hole-hole correlation energies for oxygen in the samples studied

Sample	$\Delta\alpha'$ eV	$\Delta\beta'$ eV	U(2p2p) eV	U(2s2p) eV
SiO_2				
AR	0.9	3.6	7.6	12.9
Re-ox.	0.9	3.6	7.6	12.9
Al_2O_3				
AR	0.2	4.2	8.3	12.3
Red.H_2	0.3	4.5	8.2	12.0
Ar^+ etched	0.3	4.3	8.2	12.2
Re-ox.	0.1	4.5	8.4	12.0
Fe_2O_3				
AR	3.5	8.5	5.0	8.0
Calcined	3.8	8.2	4.7	8.3
B-red.H_2	3.4	8.4	5.1	8.1
Re-ox.	4.7	8.9	3.8	7.6
Mixture M				
AR	1.6	5.8	6.9	10.7
	2.9	8.0	5.6	8.5
Re-ox				
	1.9	5.2	6.6	11.3
	3.0	7.2	5.5	9.3
ULA1AT				
AR	1.7	5.5	6.8	11.0
	4.3	8.3	4.2	8.2
SLB1 BT				
AR	0.8	4.4	7.7	12.1
Annealed	1.1	4.7	7.4	11.8
Ar^+ etched	1.1	4.5	7.4	12
Re-ox.	0.8	4.6	7.7	11.9
SLB1 AT				
AR	0.6	4.4	7.9	12.1
Ar^+ etched	0.6	4.6	7.9	11.9
Annealed	0.5	4.1	8.0	12.4
Re.ox.	0.5	4.7	8.0	11.8
VL1 AR				
Ar^+ etched	2.3	6.7	6.2	9.8
Calcined	2.4	6.6	6.1	9.9
Re-ox.	1.6	5.8	6.9	10.7
	2.3	6.3	6.2	10.2
VL1 AT				
AR				
Calcined	2.5	6.5	6.0	10
Ar^+ etched	1.8	5.8	6.7	10.7
Re-ox.	1.5	5.7	7.0	10.8
	2.3	6.1	6.2	10.4
MgO				
AR				
Re-ox.	0.4	4.3	8.1	10.2
	0.7	5.2	7.8	11.3

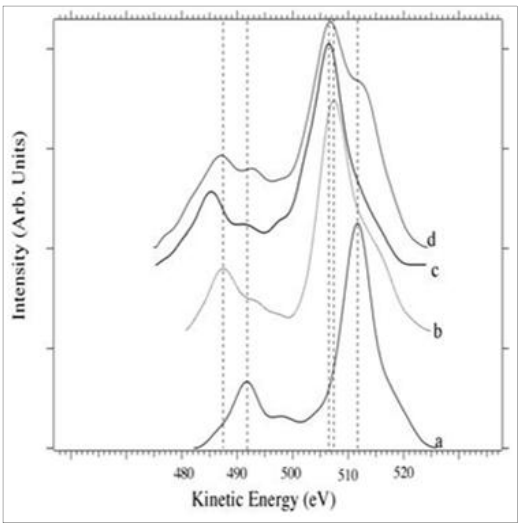

Fig. 6: O KLL Auger spectra from: a) Fe_2O_3, b) Al_2O_3, c) SiO_2 and d) mixture M.

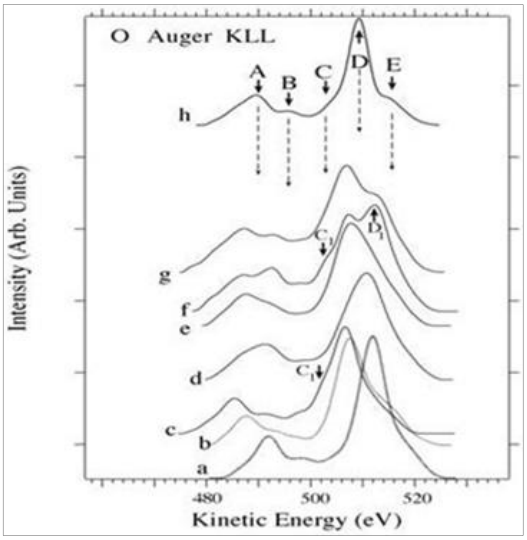

Fig. 7: Oxygen KLL Auger Spectral regions for samples: a) Fe_2O_3, b) Al_2O_3, c) SiO_2AR, d) VL1, e) SLB1, f) ULA1, AT g) Mixture M AR, h) MgO

Sample ULA1 AT

ULA1 also exhibits a differential charge effect. This effect should be taken into account when comparing Auger spectra from samples exhibiting differential charge effect and those, which have a homogenous charge effect (see figure 8). In this case ULA1 and mixture M are considered as having a homogenous charge effect to obtain a unique kinetic energy scale. This implies that the $KL_{23}L_{23}$ transition peak position from oxygen bonded to silicon (or to iron; one of the two) are fictitious depending on which value of the charge effect is used, since for these samples there are two values for the charge referencing procedure.

The C 1s spectrum, not shown here, for this sample shows a FWHM remarkably larger to that observed in Fe_2O_3, in corre spondence to the differential charge effect present on this sample[23]. No carbonates were found in this sample and the CO contribution was very low.

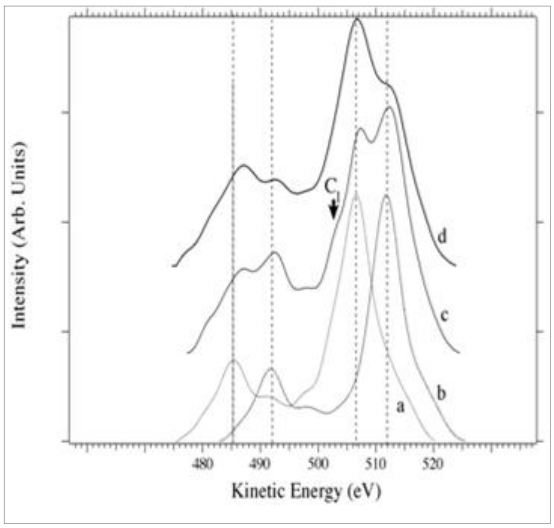

Fig. 8: A comparison among the oxygen Auger spectra for samples: a) SiO_2, b) Fe_2O_3, c) ULA1, d) mixture M.

In figure 8 the oxygen Auger spectrum of ULA1 AT (spectrum c) is compared to those of SiO_2 (spectrum a), Fe_2O_3 (spectrum b) and Mixture M (spectrum d); the differential charge effect is corrected in spectrum c according to its value in the iron region. A good correspondence is present among the peaks similar to previous reports[16], that show mainly Fe_2O_3 and SiO_2 , with no iron silicate present. Structure C_1 in figure 8 (spectrum c) and figure 7 (spectrum f) does not appear in the corresponding spectrum of the mechanical mixture (figure 8 spectrum d and figure 7 spectrum g), without resorting to a peak decomposition, probably due to the fact that in the latter sample there is a contribution from the oxygen bonded to Al_2O_3.

Auger Structures

Structures A, B, C, D in figure 7 have been assigned by Wagner[1] to the transitions: KL_1L_2 ($^1P_3$), KL_1L_3 (^3P), KL_2L_2 ($^1S_0$), and KL_2L_3 ($^1D_2$). Structure C ascribed to the KL_2L_2($^1S_0$) transition appears, according to Wagner, in ionic compounds like LiF and Na_2CrO_4. This structure is present in all the compounds studied in this report except VL1 and SLB1, and it is clear in the more covalent SiO_2 than in MgO where the structure is less sharp.

Structure E in figure 7h has been attributed, by Fuggle et al.[2], to a $KL_{23}M$ transition (where m indicates a hole in a metal like orbital) for adsorbed oxygen on metals. However, this explanation could be extended to lattice oxygen, assuming hybridization between the anionic and cationic levels. Wagner *et al.*[1] attribute this structure to OH^- groups or H_2O present. This is supported by the 20 eV energy difference between structure E and C. The energy for structure (E) does not correspond to that of OH^- species, which appears at energies between 508 eV and 510 eV and even less (503 eV) in organic compounds. If this structure corresponds to another oxygen species it should appear in the O 1s XPS peak, with low intensity due to the energy dependence of λ. Likewise,

correlation should exist between this component´s intensity and that of the Auger structure in the KVV part of the spectrum. Figures 7h and 5h show that such correlation does not exist, making Fuggle´s explanation the most probable, thus this structure´s intensity will depend on both the degree of hybridization and the involved levels occupation. In figure 7 spectrum e, representing the SLB1 oxygen Auger region, compared with VL1 (spectrum d) especially in the $KL_1L_2(^1P)$ and $KL_1L_3(^3P)$ transition regions, shows differences which indicate different chemical environments. Their Auger parameters are listed in table 1.

The energy, for the different samples, of the final state ion with two holes in level L_{23} are listed in table1 column 6; the highest value corresponds to SiO_2 and the lowest to Fe_2O_3.

Mixture M and ULA1 show the values corresponding to the presence of silicon and iron oxides. From the final state ion energy the following sequence can be established: Fe_2O_3 <VL1 < SLB1 < Al_2O_3< SiO_2. Thus, the oxygen in Fe_2O_3 has a more polarizable medium, leading to more ionic bonding, with higher charge density around oxygen, than in SLB1, etc.

Likewise, insofar as the character of the bonding to be less ionic and the covalent character increase, the difference KVV – KL_1L_{23} (table 1 column 4) increases also. The lowest value is obtained by Fe_2O_3 and the highest by SiO_2.

In the same way, in table 2 we can observe that the values of $\Delta\alpha'$ and $\Delta\beta'$ follow the same tendency, i.e. the sample with the highest final ion energy (SiO_2) should have the lowest value of $\Delta\alpha'$ and $\Delta\beta'$ and the one that has the lowest final ion energy (Fe_2O_3) will exhibit the highest values for $\Delta\alpha'$ and $\Delta\beta'$, as in fact it happens. These results are coherent with the fact that SiO_2 shows the highest values for the hole-hole correlation energies U(2s,2p) and U(2p,2p) of the final ion state, and Fe_2O_3 have the lowest values for these quantities. The values of these energies for the samples Al_2O_3, VL1, SLB1 (ULA1 and the Mixture with its two set of values) are laid between those extremes.

It can be established from tables 1 and 2 and from figures 7 and 8, that the sample sequence according to the values of the Auger parameter α' is opposed to that obtained from the values of the correlation energy U(2p,2p). In addition the sequence found by using the parameter β' is contrary to that given by the correlation energy U(2s,2p), as it should be in accordance with the definitions of these quantities[13].

Sample ordering according to α' values is not the same as that obtained using the β' parameter; since these parameters are independent of both the charge effect and the work function, thus any significant difference (beyond the experimental uncertainties), should arise from the different chemical environment effect on the levels involved in the transitions: $KL_{23}L_{23}$ for α' and KL_1L_{23} for β'. In this sense, it is interesting to point out that the sample sequence obtained according to the values of the difference KVV-KLV is nearly identical to that found by the values of the energy U(2s,2p). That difference increases as the ionicity of the oxygen bond with the corresponding cation decreases, that it is to say as the electron density on the oxygen initial state decreases, the final state ion energy increases[3].

Conclusions

The potentiality of the X-ray excited Auger electron spectroscopy has been shown once more in this work for the identification of surface chemical states in the three samples of aluminosilicates studied .

Detailed analysis of the oxygen Auger KLL region of the samples studied, allows us to distinguish the type of compounds present on samples SLB1 and VL1 from those present in samples ULA1 and the mechanical mixture. This has been achieved by obtaining information from the Auger parameters and the exploitation of the shape and the structure exhibited by the KLL region. Our study indicates the presence of some aluminate (and/or ferrate) on the surface of the VL1 sample different to that present on sample SLB1.

The Auger parameter β' involving the O 2s level with a core level and a valence level character, shows different results than when using parameter α', which only involves the 2p levels; those differences are also present in the values of the KVV-KLV difference.

Acknowledgements

The authors would like to thank Ecos- Nord (France) and CONICIT (Venezuela) for funding project ECOS V99. Thanks to Dr Labrecque for supplying the certified samples VL1 and SLB1 analyzed in this work and to Prof. B. Fontal from ULA for reading the manuscript. J.M, R.C., F.R., and A.R. thank to Mr J. C. Marchal, Mr. M. Clement from Laboratoire de Catalyse hetérogene-Univetsité de Lille I-France and Mr. J. Sarmiento from ULA for their valuable technical assistance.

References

1. CD Wagner, DA Zatko, RH Raymond. Use of the oxygen KLL Auger lines in identification of surface chemical states. **Analytical Chemistry, 52,** 1445-1451 (1980).
2. JC Fuggle, E Umbach, R Kakoschke, D Menzel. High-resolution auger spectra of adsorbates. **J. Electron Spectroscopy and Related Phenomena, 26**, 111-132 (1982).
3. CD Wagner, DJ Passoja, HF Hilleray, TG Kinisky, HA Six, WT Jansen, JA Taylor. Auger and photoelectron line energy relationships in aluminum-oxygen and silicon-oxygen compounds. **J. Vac. Sci.Technol., 21,** 933-944 (1982).
4. JE Castle, RH West. Bremsstralung-Induced Auger Peaks. **J. Electron Spectrosc. Relat. Phenom., 18,** 355-358 (1980).
5. RH West, JE Castle. The correlation of the Auger Parameter with refractive index: An XPS study of Silicates using Zr-Lα Radiation. **Surface and Interface Analysis, 4,** 68-75 (1982).

6. JC Riviere, JA Crossley. Study of interfaces in oxidized fe/Si ststem by XPS and XAES: Use of the Auger parameter. **Surf. Interface Anal., 8,** 173-181 (1986).

7. CD Wagner. Chemical Shifts of Auger Lines and the Auger Parameter. **Faraday Discussions of the Chemical Society, 60**, 291-300 (1975).

8. CD Wagner CD. Auger Parameter in Electron Spectroscopy for the Identification of Chemical Species. **Anal. Chem., 47**, 1201-1203 (1975).

9. CD Wagner, A Joshi. The Auger Parameter its utility and advantages: A review. **J. Electron Spectrosc. Relat. Phenom. 47,** 283-313 (1988).

10. SW Gaarenstroom, N. Winograd. Initial and final state effects in the ESCA spectra of cadmium and silver oxides. **J. Chemical Physics, 67**, 3500-3505 (1977).

11. CD Wagner, LH Gale, RH Raymond. Two-Dimensional Chemical State Plots: A Standardized Data Set for Use in Identifying Chemical States by X-Ray Photoelectron Spectroscopy. **Anal. Chem., 51(4)**, 466-482 (1979).

12. JC Riviere, JA Crossley, G Moretti. Core-Level Shifts and the Choice of Auger Parameter. **Surf. Interface Anal., 14,** 257-266 (1989).

13. G Moretti. The use of the oxygen Auger Parameter in the characterization of oxygen-containing compounds. **J. Electron Spectrosc. Relat. Phenom., 58**: 105-118 (1992).

14. G Moretti. Auger Parameter and Wagner plot in the characterization of chemical states by X-ray photoelectron spectroscopy: a review. **J. Electron Spectrosc. Relat. Phenom., 95**, 95-144 (1998).

15. J Mendialdua, R Casanova, Y Barbaux. XPS studies of V2O5, V6)13, VO2 and V2O3. **J. Electron Spectrosc. Relat. Phenom., 71,** 249-261 (1995).

16. A Loaiza, B Fontal, F Rueda, J Mendialdua, R Casanova. On carbonaceous deposit formation in carbon monoxide hydrogenation on a natural iron catalyst. **Applied Catalysis, A177,** 193-203 (1999).

17. J Mendialdua, R Casanova, FbRueda, A Rodríguez, J Quinones, L Alarcon, E Escalante, P Hoffmann P, I Taebi, L Jalowiecki. X-ray photoelectron spectroscopy studies of laterite standard reference material. **J. Mol. Catalysis, A228**, 151-162 (2005).

18. F Rueda, J Mendialdua, A Rodríguez, R Casanova, Y Barbaux, L Gengembre, L Jalowiecki, D Bouqueniaux. Quantitative XPS studies of a natural catalyst. **J. Electron Spectrosc Relat. Phenom. 70**, 225-231 (1995).

19. G Ertl, J Kuppers. Low Energy Electron and surface Chemistry. Verlag Chemie, GmbH, D-694 Weinheim, pp 25-29 (1974).

20. H Schorim, JLabrecque. A Larerite Standard Reference Material VL-1. **Geostandards Newsletter, 7(1)**, 233-242 (1983).

21. J Labrecque, H Schorim. Certification of SLB-1, a Suriname lateritic bauxite material as a standard reference material. **Fresenius J. Anal. Chem., 342**, 306-311 (1992).

22. F Rueda. Doctoral Thesis. Universite des Sciences et Technologies de Lille. France (1997).

23. F Rueda, J Mendialdua, A Rodríguez, R Casanova, Y Barbaux, L Gengembre, L Jalowiecki. Characterization of Venezuelan laterites by X- ray photoelectron spectroscopy. **J. Electron Spectrosc Relat. Phenom., 82,** 135-143 (1996).

24. F Rueda, J Mendialdua, A Rodríguez, R Casanova, Y Barbaux, L Gengembre, L Jalowiecki, D Bouqueniaux. Inhomogeneous charge effect on a natural mineral studied by XPS. **Surf. Interface Anal., 21**, 659-664 (1994).

25. J Mendialdua. Ph.D thesis, number 559. Université de Sciences et Techniques de Lille. France (1983).

26. L Jalowiecki. Université de Sciences et Techniques de Lille. France. Technical Report ECOS-Nord Project PI 99000235 (2001).